



저작자표시-비영리-변경금지 2.0 대한민국

이용자는 아래의 조건을 따르는 경우에 한하여 자유롭게

- 이 저작물을 복제, 배포, 전송, 전시, 공연 및 방송할 수 있습니다.

다음과 같은 조건을 따라야 합니다:



저작자표시. 귀하는 원저작자를 표시하여야 합니다.



비영리. 귀하는 이 저작물을 영리 목적으로 이용할 수 없습니다.



변경금지. 귀하는 이 저작물을 개작, 변형 또는 가공할 수 없습니다.

- 귀하는, 이 저작물의 재이용이나 배포의 경우, 이 저작물에 적용된 이용허락조건을 명확하게 나타내어야 합니다.
- 저작권자로부터 별도의 허가를 받으면 이러한 조건들은 적용되지 않습니다.

저작권법에 따른 이용자의 권리는 위의 내용에 의하여 영향을 받지 않습니다.

이것은 [이용허락규약\(Legal Code\)](#)을 이해하기 쉽게 요약한 것입니다.

[Disclaimer](#)

Master's Thesis

Applicability of Fitts' Law in VR Environment:
Effects of Incline Angle, Azimuth Angle, and
Muscle Fatigue on Speed-Accuracy Tradeoff

Minjoong Kim

Department of Human Factors Engineering

Graduate School of UNIST

2019

Applicability of Fitts' Law in VR Environment: Effects of Incline Angle, Azimuth Angle, and Muscle Fatigue on Speed-Accuracy Tradeoff

Minjoong Kim

Department of Human Factors Engineering

Graduate School of UNIST

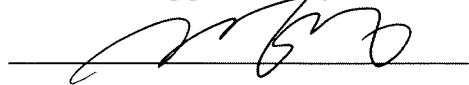
Applicability of Fitts' Law in VR Environment: Effects of Incline Angle, Azimuth Angle, and Muscle Fatigue on Speed-Accuracy Tradeoff

A thesis
submitted to the Graduate School of UNIST
in partial fulfillment of the
requirements for the degree of
Master of Science

Minjoong Kim

01. 07. 2019

Approved by



Advisor


Gyouhyung Kyung, Ph.D.

Applicability of Fitts' Law in VR Environment: Effects of Incline Angle, Azimuth Angle, and Muscle Fatigue on Speed-Accuracy Tradeoff

Minjoong Kim

This certifies that the thesis of Minjoong Kim is approved.

01/07/2019



Advisor: Gyouhyung Kyung, Ph.D.



Thesis Committee Member: Gwanseob Shin, Ph.D.



Thesis Committee Member: Ohsang Kwon, Ph.D.

Abstract

With recent advancements in computer technologies, the advanced virtual reality (VR) technologies are available in the market at a reasonable price for everyone, allowing even novice users to experience the first-person virtual environment for entertainment and training. The performance evaluation in a virtual environment is important to provide guidelines for designing user interfaces (UI) and interaction methods for diverse VR contents. As the Fitts' law has been used as a tool to evaluate UI in the field of Human Computer Interactions (HCI), the application of Fitts' law for interactive VR contents design is inevitable. Because the virtual world created by VR technologies is not so realistic as the real world, it is questionable whether the Fitts' law that can be used for plain 2D movement to complex motor control in the real world will still hold in VR.

Although there have been multiple studies involving Fitts' law in VR, most of them were limited in 2D or ray-casting/remote pointing techniques which represent only a fragment of possible interactions in both real world and virtual world. With right VR input devices, it is possible to reproduce even more direct and physical interactions in a 3-dimensional level that represent the tactile interactions in the real world. Hence, for this research, an existing real-world 3D Fitts' law test was regenerated in the VR environment with some modifications considering the hardware limitations of the Head Mount Display (HMD) device. In addition to movement time and error occurrence, subjective and physiological muscle fatigue measures were obtained to examine the effect of muscle fatigue on the performance of non-reciprocal pointing and grasping tasks in the VR environment because muscle fatigue can affect the usage time of experience-based contents.

A total of 12 male individuals (right-handed, not wearing glasses, and having no stereopsis disorder) participated in this study. The virtual environment used in this study was designed using UNITY and presented using HTC Vive. The Fitts' law task involved simple pointing and grasping (by pulling the trigger on the controller) on a target which appeared as soon as participants successfully acquired the starting point object. The task was designed with 3 levels of target width (0.015m, 0.03m, and 0.06 m), 3 levels of amplitude (0.05m, 0.1m, and 0.15m), 8 levels of azimuth angle (0 °, 45 °, 90 °, 135 °, 180 °, 225 °, 270 °, and 315 °), and 3 levels of incline angle (30 °, 60 °, and 90 °), leading to a total of 216 treatments. The presentation order within each trial was completely randomized. Participants were instructed to acquire targets as fast and accurate as possible. Participants completed 3 sets (trials) of these treatments during the main experiment, following one full trial during a practice session. Failing to grasp a target for a given treatment was counted as an error. Error-induced treatments reappeared in random order at the end of the trial until there was no error in the trial.

Movement time was defined as a time length between the moment to acquire the starting point and the moment to grasp the target object. Participants reported their perceived fatigue level of each

muscle part on the Borg CR-10 scale pre and post-trial. In addition, electromyographic (EMG) signals from the bicep brachii and anterior deltoid were measured throughout each trial to assess muscle fatigue.

The movement time of all participants was averaged by each treatment level and then analyzed to find the regression model concerning the index of difficulty (calculated using target width and amplitude), incline angle, and azimuth angle. EMG signal was analyzed by transforming the signal into Root Mean Square (RMS) value and median frequency (MDF) value to observe the physical muscle fatigue for each trial.

Regression analysis showed a significant effect of azimuth angle ($p = 0.038$) while there was no significant effect of the index of difficulty (ID; $p = 0.66$). The Borg scale of muscle fatigue clearly showed an increase in muscle fatigue for the anterior deltoid muscle ($p < 0.0001$) as well as the bicep brachii muscle ($p < 0.0001$). However, none of the physiological values showed a significant effect of the trial progress, potentially due to the light weighted controller (200 g), yet still, the subjective measure significantly increased from trial 1 to trial 3.

Overall, low R^2 values and non-significant results for the independent variables considered in this study except the azimuth angle indicate that Fitts' law does not strongly hold in VR. The result of this study can be utilized when designing more specific Fitts' law tasks to test Fitts' law regarding specific variables involving the positional data of targets. The ranges of the independent variables were limited due to hardware limitations such as the field of view of the HMD. A novel approach to overcome such a limitation is warranted to further assess the applicability of Fitts' law in VR in the future. Additionally, only the muscle fatigue of the anterior deltoid and bicep brachii rated on Borg's scale showed significant effects between trials, whereas the EMG data showed no significant differences between trials. Additionally, a speed-accuracy tradeoff was observed across trials (increase in speed and decrease in accuracy), indicating the need of including muscle fatigue as a potential parameter for a new Fitts' law model, especially for the VR environment.

Table of Contents

Abstract	I
List of Figures	V
List of Tables	VI
I. Introduction	1
II. Methods	7
2.1 Participants	7
2.2 Experimental apparatus	7
2.3 Experimental environment	9
2.4 Experimental design	9
2.4.1 Independent variables	12
2.4.2 Dependent variables	14
III. Results	15
3.1. Fitts' Law	15
3.2. Muscle Fatigue	18
IV. Discussion	20
4.1 Fitts' Law	20
4.1.1 Index of Difficulty	21
4.1.3. Azimuth angle	22
4.2 Muscle Fatigue	25
V. Conclusion	27
References	28

List of Figures

Figure 1. Experimental setting of (Murata and Iwase, 2001) -----	6
Figure 2. (a) incline angle and (b) azimuth angle expressed by Cha and Myung (2013) -----	6
Figure 3. Schematic of the experimental setup by Cha and Myung (2013) -----	6
Figure 4. HTC Vive-----	8
Figure 5. PolyG-I -----	8
Figure 6. RANDOT Stereo Test-----	8
Figure 7. Experimental environment and apparatus-----	10
Figure 8. Participant performing the experiment -----	11
Figure 9. The scene of the experiment-----	11
Figure 10. Incline angle layout from the participant's point of view-----	13
Figure 11. Azimuth angle layout from the front view -----	13
Figure 12. EMG surface electrode attached on bicep brachii and anterior deltoid-----	13
Figure 13. Average movement time as a function of (a) amplitude, (b) target width, (c) incline angle, and (d) azimuth angle.-----	16
Figure 14. Average movement time vs. average error occurrence for each trial-----	18
Figure 15. Fatigue of bicep brachii and anterior deltoid comparisons by (a) Borg RPE Scale, (b) normalized RMS, and (c) MDF -----	19
Figure 16. Regression of average movement time by the index of difficulty ($p = 0.104$) -----	22
Figure 17. Movement time by azimuth angle at each level of (a) incline angle, (b) amplitude, and (c) target width-----	24

List of Tables

Table 1. Borg's CR-10 Scale (Borg, 1998) -----	5
Table 2. Parameters estimates (a: intercept, b: sigmoid of azimuth angle, c: cosine of incline angle, d: index of difficulty) and the p-value from effect test of each parameter -----	17
Table 3. Mean (SD) Borg RPE Scale, normalized RMS (median), and MDF (median) values of Bicep Brachii and Anterior Deltoid on each trial.-----	19
Table 4. The post-hoc analysis result of the effect of the trial on movement time and error occurrence -----	20
Table 5. Index of difficulty levels and range comparison between current and previous Fitts' Law studies -----	21
Table 6. ANOVA result to test the effect of incline angle and target width on movement time -----	22
Table 7. Effect test result using the sinusoidal function of azimuth angle instead of sigmoid -----	23
Table 8. Tukey's HSD result on sinusoidal function and sigmoid function of azimuth angle (post hoc analysis)-----	23
Table 9. ANOVA result on trial effect on muscle fatigue -----	26
Table 10. Post-hoc analysis of the trial effect on Borg's scale on bicep brachii -----	26
Table 11. Post-hoc analysis of the trial effect on Borg's scale on anterior deltoid -----	26

I. Introduction

With the recent development of virtual reality (VR) technology, the application of virtual platforms and interaction in the virtual environment is advancing every day, and diverse VR applications are available in the market for end users to purchase and experience. The main applications of current VR platforms are focused on entertainment, yet VR applications in other fields (e.g., training and medicine) and as a medium to deliver a new experience are rapidly increasing and expected to become a primary method of interaction and communication in the future. Given that the safety and efficiency of VR technology are still uncertain, the evaluation of both VR health and performance under the virtual environment considering its technological limitations are yet to be analyzed (Steuer, 1991; Biocca, 1992). There have been multiple studies involving visually stimulated sicknesses (Dichgans & Brandt, 1978; Hettinger & Riccio, 1992; Arsenault & Ware, 2004) caused by a mismatch between visual perception and physical movement. Also, performance-related studies have been conducted regarding the effect of presence (Slater, Usoh, & Steed, 1995; Schuemie, Van Der Straaten, Krijn, & Van Der Mast, 2001; Sanchez-Vives & Slater, 2005) and motor control in VR (Decety & Jeannerod, 1995; Liu, van Liere, Nieuwenhuizen, & Martens, 2009). However, there are relatively fewer studies on the performance in VR respect to muscle fatigue. Studies on muscle fatigue either ended up only suggesting the need of muscular fatigue data (Kiryu & So, 2007; Pontonnier, Dumont, Samani, Madeleine, & Badawi, 2014) or designing a VR framework to apply the fatigue index to the virtual environment using a new dynamic muscle fatigue model (Ma, Chablat, Bennis, & Zhang, 2009).

The Fitts' law has been used commonly in previous studies involving VR to either measure the performance of interaction methods (Johnsgard, 1994; Ware & Lowther, 1997; Ahlström, 2005; Das & Borst, 2010; Teather, Natapov, & Jenkin, 2010; Ramcharitar & Teather, 2017; Hansen, Rajanna, MacKenzie, & Bækgaard, 2018) or the effect of hardware limitations such as lag and frame rates (MacKenzie & Ware, 1993; Ware & Balakrishnan, 1994a, 1994b). There have been attempts to assess Fitts' law into the virtual environment by multiple researchers using various input devices to interact in the virtual environment. Most of them used indirect interaction methods such as point techniques using gaze (Ware & Lowther, 1997; Hansen, Rajanna, MacKenzie, & Bækgaard, 2018), ray-casting (Das & Borst, 2010), game controllers (thumbstick, touchpad, and gyrosensor; Ramcharitar & Teather, 2017), or to analyze the effect of haptic feedback (Teather, Natapov, & Jenkin, 2010). Johnsgard (1994) conducted a direct comparison between virtual reality gloves and computer mouse; however, the purpose of this study was to test the effect of gain on movement speed. Hence, even though Fitts' law model or tasks have been implemented in VR or virtual environment, the applicability of Fitts' law model was not tested in the advanced representation of the real world. Most of the studies were conducted using stereo-capable monitors (MacKenzie & Ware, 1993; Ware & Balakrishnan, 1994a,

1994b; Ware & Lowther, 1997; Liu, van Liere, Nieuwenhuizen & Martens, 2009;) or cave automatic virtual environment (CAVE), the spatial VR using projectors to project images on the wall (Teather, Natapov, & Jenkin, 2010). Hence, the applicability of Fitts' law model in a life-like virtual environment using advanced technology with the input device that can provide a 1:1 gain ratio and no limitation on the movement range is yet to be fully verified.

To evaluate the interaction in the virtual environment, the determination of similarity between real-world physical movement and the movement in the virtual environment is essential. For this purpose, the analysis of the movement in the virtual environment needs to be assessed using Fitts' law. Fitts' law was found by Paul M. Fitts in 1954 as he conducted a series of studies to analyze the information capacity of the human motor system in controlling the amplitude of movement (Fitts, 1954). Fitts used a conventional information notation called index of difficulty (ID) to estimate the movement time (MT) to acquire a target from a given starting point (Fitts, 1954). After a series of research, Fitts proposed a model that predicts the time it takes to reach a target at a given length between the starting point and the center of the target (Amplitude) and the size of the given target (Width). The original Fitts' Law model is shown in Equation 1 (Fitts, 1964). Coefficients a and b in the model are the empirical constants depending on the choice of input device. The ID of his original work is a log function of the target width (W) and amplitude (A) (Equation 2).

$$MT = a + b ID \quad (1)$$

$$ID = \log_2\left(\frac{2A}{W}\right) \quad (2)$$

The ID used in the original Fitts' Law has a major problem caused by the nature of a log function; when the width of the target is twice as wide as the amplitude, the ID value returns a negative value. Many researchers have come up with modified versions of the index of difficulty. The most well-known and widely adopted variation is by Welford (1960; 1968; Equation 3) derivative of Shannon's original theorem. Then, the direct analogy with Shannon's information theorem variation of the index of difficulty was suggested (Equation 4; Mackenzie, 1992). Hoffman (1991, 1995) introduced a variation of index of difficulty including the size of the probe (e.g., finger) (Equation 5).

$$ID = \log_2\left(\frac{A}{W} + 0.5\right) \quad (3)$$

$$ID = \log_2\left(\frac{A}{W} + 1\right) \quad (4)$$

$$ID = \log_2\left(\frac{2A}{W + F}\right) \quad (5)$$

The original Fitts' law tasks were 1-dimensional tasks, where a starting point and targets are aligned in a single line, with regarding only the width of the target regardless of how tall the target is, then the Fitts' law was applied for 2-dimensional tasks, and the definition of target width changed. The variations of target width are the minimum of width and height, the apparent width in the direction of motion, the sum of target width and height, the product of target width and height, and the target width itself as the original Fitts' Law (Accot & Zhai, 2003).

Then, the researchers started to take the Fitts' law model to the next level. Three-dimensional Fitts' law models were developed. Murata & Iwase (2001) have developed a Fitts' law model by implementing 3-dimensional task; the 2D circular targets were placed on a plane in a concentric circle phased by 45°, the distance of the plane was adjusted along the x-axis as in term of depth (distance from the participant; Figure 1). The revised ID used in the study by Murata & Iwase (2001) is shown as Equation 6. Although Murata & Iwase (2001) have successfully tested and modified ID with semi 3D task, there were still limitations in their study: first, the targets were 2D targets in a flat plane; second, the function of the depth of the target location (or the distance from origin along the x-axis; Figure 1) was not implemented into the ID.

$$ID = \log_2\left(\frac{A}{W} + 1\right) + c \sin \theta \quad (6)$$

From the study of Murata and Iwase (2001), Cha & Myung (2013) have conducted a more advanced 3D Fitts' law task by introducing the incline angle into the Fitts' law model (Figure 2). 2D square targets were arranged by 8 levels of azimuth angles (0°, 45°, 90°, 135°, 180°, 225°, 270°, and 315°) around the circular starting point in the center adjusted by a magnet to predetermined 3 levels of incline angles (30°, 45°, and 60°; Figure 3). The modified Fitts' law model developed using 3 levels of target width (1cm, 2cm, and 3cm), 4 levels of amplitude (30cm, 40 cm, 50cm, and 60cm), 3 levels of incline angle (θ_1), and 8 levels of azimuth angle (θ_2) with the ID introduced by Hoffman (1995; equation 5) is expressed as equation 7.

$$MT = a + b\theta_1 + c \sin(\theta_2) + d \log_2\left(\frac{A}{W + F}\right) \quad (7)$$

While testing the applicability of Fitts' law, as the virtual tasks develop, the performance evaluation in the virtual environment is also important for future application of virtual interaction. As users perform multiple interaction motions for a long period, the increase of muscle fatigue is inevitable, and the increase in muscle fatigue can affect the performance (movement speed and accuracy) of

pointing or direct object acquiring tasks. Therefore, the effect of fatigue as in term of repetition of Fitts' law task on the movement time and the number of error occurrences must be analyzed, and if possible, by taking the magnitude of muscle fatigue as a parameter in Fitts' law model. Muscle fatigue can be assessed either subjectively or physiologically (e.g., electromyogram; EMG).

The subjective measure of muscle fatigue can be measured as the level of exertion, the rating of perceived exertion (RPE) that a person perceives to be required to perform a given task. Borg RPE scale is commonly used to measure a subjective level of exertion (fatigue) for a given task (Borg, 1998). The EMG signals can be used to assess muscle fatigue using amplitude and frequency-based analysis. As muscular fatigue increases, the amplitude also increases, whereas the mean or median frequency of total power spectrum decreases (Konrad, 2006). Park, Hong, & Lee (2012) conducted a Fitts' law task experiment on a remote pointing technique while using an upper-arm support to reduce muscle fatigue. Borg's CR-10 scale was used to measure subjective fatigue along with EMG on the upper trapezius and anterior deltoid. Mean power frequency (MPF), median frequency (MDF), and the root means square (RMS) was derived from EMG data to analyze muscle fatigue (Park, Hong, & Lee, 2012).

The purpose of this thesis was to examine the applicability of Fitts' law in the virtual environment and to analyze the effect of muscle fatigue in term of subjective and physiological muscle fatigue measures, to see how the increase in muscle fatigue affects the performance of Fitts' law task. The Fitts' law task in this experiment was designed by 3 levels of widths and amplitudes resulting a total of 7 levels of an index of difficulty along with the 8 levels of azimuth angles and 3 levels of incline angles. The starting and target objects were sphere-shaped to keep the target width constant regardless of the approaching angle each participant may take. The performance level of the Fitts' law task was measured by movement time (ms) and error occurrences (number of errors per trial). Participants performed 3 trials of a full set of treatments to observe the effect of fatigue, and the muscle fatigue was assessed using Borg's CR-10 scale (subjective measure) and EMG (physiological measure).

Table 1. Borg's CR-10 Scale (Borg, 1998)

Rating	Description
0	Nothing at all
0.5	Very very light
1	Very light
2	Fairly light
3	Moderate
4	Somewhat hard
5	Hard
6	
7	Very hard
8	
9	
10	Very very hard (Maximal)

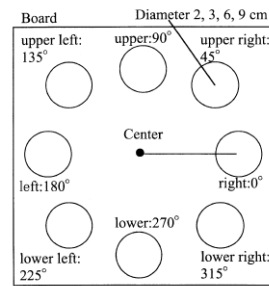


Fig. 2. Array of targets on the board used in the experiment.

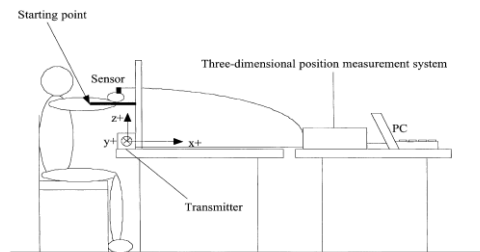


Fig. 3. Outline of experimental setup (see text for details).

Figure 1. Experimental setting of Murata and Iwase (2001)

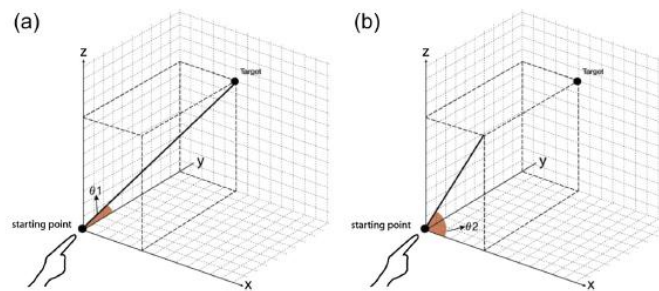


Figure 2. (a) Incline angle and (b) azimuth angle expressed by Cha and Myung (2013)

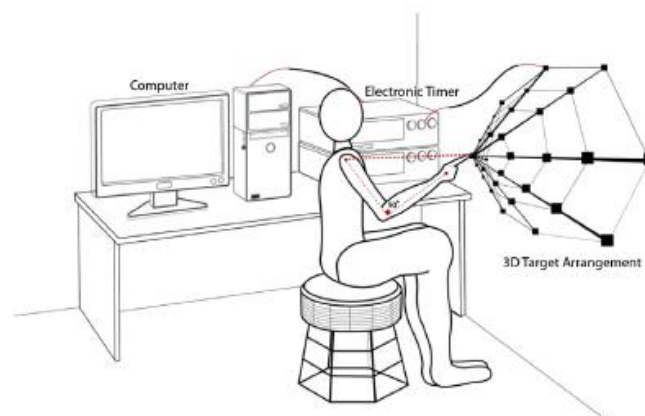


Figure 3. Schematic of the experimental setup by Cha and Myung (2013)

II. Methods

2.1 Participants

A total of 12 right-handed male individuals with the age range of 18-27 years old participated in this study. The mean (SD) age of participants was 23.3 (2.5). All participants were recruited from the university population, wore no glasses, and reported no musculoskeletal diseases on their upper limbs. To make sure that none of the participants had a problem recognizing virtual objects in virtual reality (VR), each participant was tested with Stereo Test by RANDOT[®] for stereopsis disorder. All participants passed the Stereo Test with no sign of stereopsis disorder with the mean (SD) score of RANDOT Stereo Test of 114.2 (60.4) arcsec.

2.2 Experimental apparatus

The program for testing Fitts' Law in VR was developed using Unity ver. 5.6.1 (Unity Technology, U.S.A.) and SteamVR Plugin Ver. 1.2.3 (Valve Corporation, U.S.A.). Participants performed Fitts' Law tasks using HTC Vive (HTC, Taiwan; Figure 4), the virtual reality head mounted display designed by HTC. HTC Vive provided a horizontal field of view of 110° and vertical field of view of 100°, providing images through Dual 3.6" AMOLED display at a refresh rate of 90 Hz. The standard controller of HTC Vive (weight: 203 g) was used for participants to interact in the virtual environment. HTC Vive was hooked up to the VR Ready computer with 4.5GHz Intel Core i7-7700K CPU (Intel Corporation, U.S.A.), dual channel Samsung DDR4 16GB PC4-19200 RAM (Samsung, Korea), and graphic card of Geforce GTX 1080 Ti AORUS Xtreme D5X 11GB (Gigabyte Technology, Taiwan). EMG signal was collected using PolyG-I (Laxtha, Korea; Figure 5) at the rate of 512 Hz hooked up to the same computer that was connected to the HTC Vive. Perceived muscle fatigue was verbally rated on Borg rating of perceived exertion (RPE) scale (Borg, 1998; Table 1). For the data analysis, SAS JMP Pro 14 (SAS Institute Inc., U.S.A.) and MATLAB R2018b (MathWorks, U.S.A.) were used.



Figure 4. HTC Vive



Figure 5. PolyG-I



Figure 6. RANDOT Stereo Test

2.3 Experimental environment

The participants were seated on a chair for experiment between two HTC Vive base stations used to capture the movement of HMD and controller within the area between the base stations. The PolyG-I was placed next to the participant to attach EMG electrodes to the participants' arm while avoiding interference of the electrode wires with the arm movements during the Fitts' Law task (Figures 7 & 8). The room setting calibration was conducted by the basic HTC Vive program provided by Valve Corporations. The room setting calibrated the center position between placed base stations and the starting height of the HMD (calibrated to be 0 m by placing HMD on the ground). The same room setting was applied to all participants.

2.4 Experimental design

Before beginning the experiment, each participant was tested with RANDOT Stereo Test, then the participants with no stereopsis disorder (no one excluded) were informed about the experiment purposes and the Borg RPE Scale. Then, participants changed to the provided t-shirt, and EMG electrodes were attached on the bicep brachii muscle, the most fatigued muscle part claimed by three participants in a pilot study, and the anterior deltoid muscle, the muscle part that bears the most load to move the elbows on remote pointing tasks (Park, Hong, & Lee, 2012). After the electrodes were attached, the participants were asked to wear the HTC Vive HMD, and adjust the focus of the lenses.

The virtual environment of the experiment is shown in Figure 9; participants were to be facing a gray color wall and dark gray floor, then participants were asked not to move for 5 seconds to find the average center position of the HMD. Then the starting point object appeared 33.7 cm away from the determined average center point. Once the participant touched the starting object with the controller probe and pulled the trigger, the start time was recorded, and the start point object disappeared, and the target object appeared in random order. The starting and target objects each was a sphere to maintain the same target width regardless of the approaching angle. Once the participant successfully acquired the target by the controller probe and pulled the trigger again, the end time was recorded, and the target object disappeared, and the start point object reappeared in the same position. Then, the difference between the end time and the start time was calculated and stored to be saved into a CSV file format later. The tactile feedback as in vibration of the controller was provided when the touch probe on the controller collided with the virtual object. For error cases, which occurred when participants failed to acquire the target and pulled the trigger, the given treatment was restored into the sequence and reappeared in random order until the all target treatments were successfully acquired. The mean (SD) period of trial 1, 2 and 3 were 6.75 (1.06) min, 5.9 (0.9) min, and 5.6 (0.79) min.

There were four independent variables (IV) in this experiment, target width and target

amplitude (3 levels each, used to calculate the index of difficulty), incline angle (3 levels), and azimuth angle (8 levels). There was a total of 216 treatments of IVs. Each participant completed one full cycle of treatments for practice, then began the main experiment. Participants reported their subjective muscle fatigue level before the main experiment on Borg's RPE scale. There was a total of 3 set of trials in the main experiment. Each trial consisted of one full cycle of 216 treatments (plus error trials). Participants completed the trials in series without a recess except for a brief pause between trials to report their subjective muscle fatigue for bicep brachii and anterior deltoid (approximately 5 seconds). Participants could quit whenever they felt too much fatigue or pain on their right upper limb. No participants quit in the middle of the experiment. EMG signals were collected continuously throughout each trial. The Borg's RPE scale and EMG data were later used to determine the muscle fatigue at each trial.

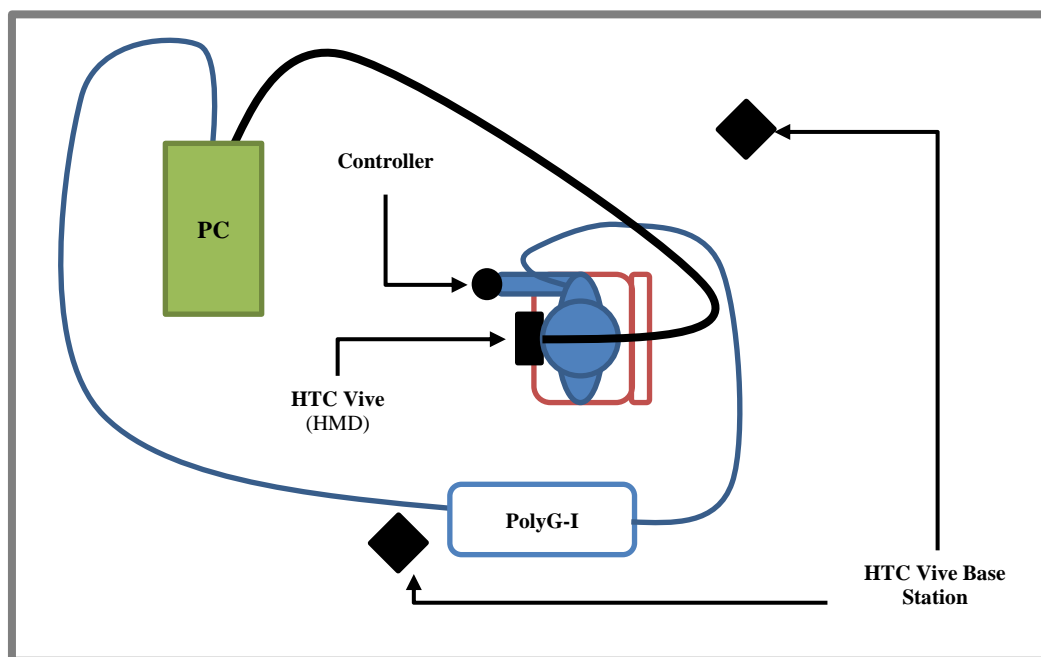


Figure 7. Experimental environment and apparatus

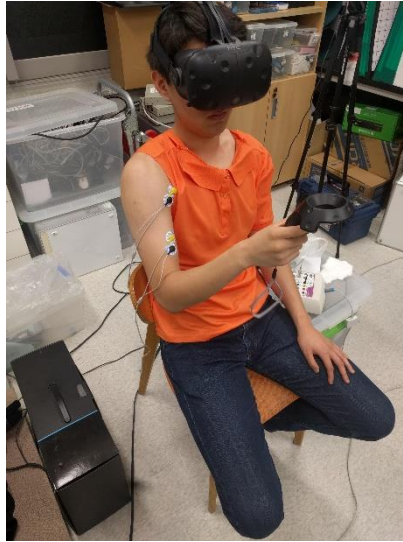


Figure 8. Participant performing the experiment

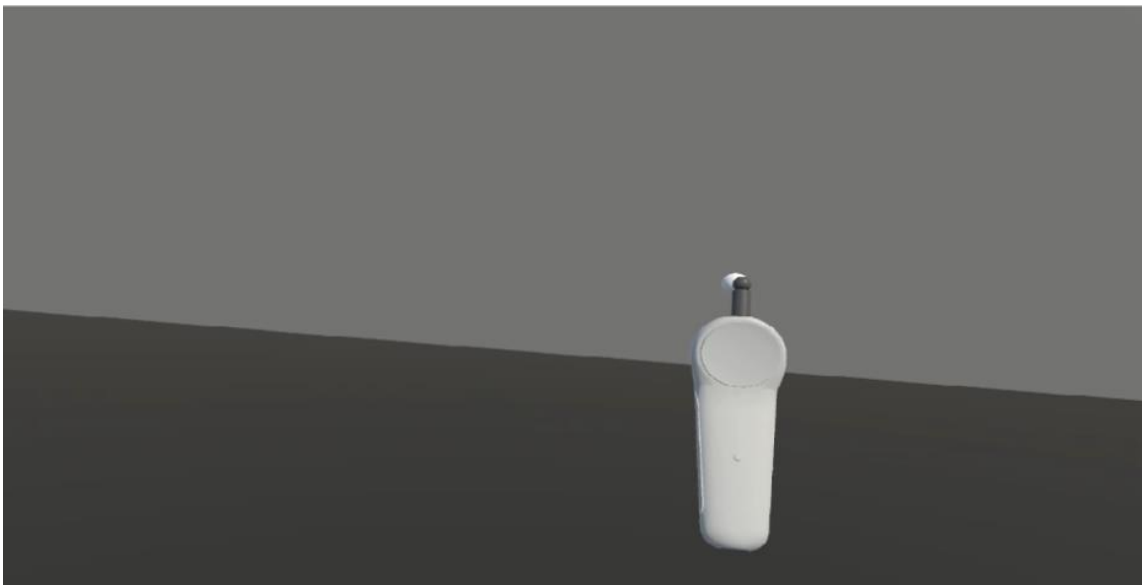


Figure 9. The scene of the experiment

2.4.1 Independent variables

Index of difficulty

The index of difficulty (ID) of the Fitts' Law was calculated using the width of the target and the amplitude between the starting point and the center of the target. For this experiment, there were three levels of width (1.5cm, 3cm, and 6cm) and amplitude (5cm, 10cm, and 15cm) calculated for targets to fall within the field of view of HTC Vive while participants could reach them without leaning their upper body and see the target without moving their head around. The original Fitts' version of ID (Equation 2) was used to calculate the ID used in this experiment since the width and amplitude used for this experiment did not return negative ID values. The ID values calculated using the widths and amplitudes above are 0.74, 1.74, 2.32, 2.74, 3.32, 3.74, and 4.32 bits. Out of 216 treatments, 120 treatments had the ID of 0.74, 2.32, 3.32, 3.74 and 4.32 (24 treatments each), and the remaining 96 treatments had the ID of 1.74 and 2.74 (48 treatments each).

Incline angle

Incline angle is the angle between the y-axis and the vector to the center of the target from the starting point while the y-axis is perpendicular to the plane that the participant faces (Figure 10). Incline angle indicates the depth of the target respect to the amplitude of the target. In this experiment, there were three incline angles: 30°, 60°, and 90°. When the incline angle was used as a variable to calculate the Fitts' Law equation, the cosine value of the incline angle was explicitly implemented to indicate the depth of the target location respect to the starting point.

Azimuth angle

Azimuth angle represents the angle between the x-axis and the target location on the x-z plane as shown in figure 11, indicating the relative location compared to the starting point. Eight levels of azimuth angle were used for this experiment: 0°, 45°, 90°, 135°, 180°, 225°, 270°, and 315°. Azimuth angle showed a possible effect of gravity influencing the movement time (Cha & Myung, 2013). Cha & Myung's work showed that the movement time change along the azimuth angle was similar to a sinusoidal wave; hence they implemented the azimuth angle in the form of sine value to the Fitts' Law in their study. However, the way human exerts force is similar to a sigmoidal wave, slowly increasing from minimal effort to gradually decreasing around the maximal level (Troiano, Naddeo, Soso, Camarota, Merletti, & Mesin, 2008). Hence for this experiment, the sigmoid value of azimuth angle was additionally analyzed and compared to the sine value of the azimuth angle.

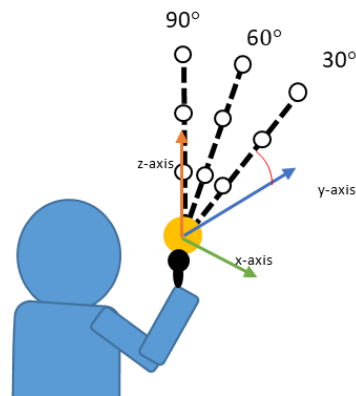


Figure 10. Incline angle layout from the participant's point of view

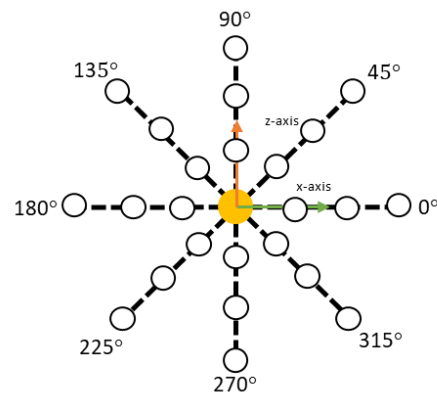


Figure 11. Azimuth angle layout from the front view



Figure 12. EMG surface electrode attached on bicep brachii and anterior deltoid

2.4.2 Dependent variables

Movement Time

The movement time was measured in milliseconds and later used to calculate Fitts' Law model through regression analysis. The movement time was calculated by the time stamps when the participant successfully acquired the starting point object and the target object, and later analyzed using regression for calculating the Fitts' Law model.

Muscle Fatigue

Muscle fatigue of bicep brachii and anterior deltoid was measured in two methods: Borg RPE scale (subjective measure) and EMG. Borg RPE scale used for this experiment was CR-10 scale (Table 1), it was measured 4 times per participant as each participant responded their subjective muscle fatigue level of each muscle before the main experiment begin and after each trial. EMG signal was collected continuously throughout the main experiment trials using PolyG-I. The disposable EMG surface electrodes were attached on bicep brachii and anterior deltoid muscles longitudinal to the direction of muscle fiber with 30 mm distance between electrodes (Figure 12). Muscle fatigue can be represented using both amplitude and frequency-based analysis. For amplitude analysis, EMG signals were calculated into time domain RMS values, and as for the frequency analysis, EMG signals were converted into the absolute values of frequency domain median frequency (MDF) data using Fast Fourier Transform (FFT) algorithm. The beginning and end timestamps of each participant's trials were recorded to select the EMG data segment for each trial. First and last 0.5 min (30 seconds) of each trial was removed, then the EMG data was processed using root mean square value to analyze the amplitude of the EMG signal. The median of RMS value was selected as the amplitude for EMG signal, and the median RMS value was normalized using the median RMS value of each participant's first 30 seconds data of the trial 1 that was removed (Park, Hong, & Lee, 2009). MDF data was calculated using the same timestamp data of EMG as RMS, then the median frequency value of each trial was compared to see the frequency shift to determine the change in muscle fatigue (Konrad, 2006). EMG signal was filtered using a band pass filter with 10Hz high-pass and 500Hz low pass frequencies to be processed into RMS and MDF values using MatLab.

III. Results

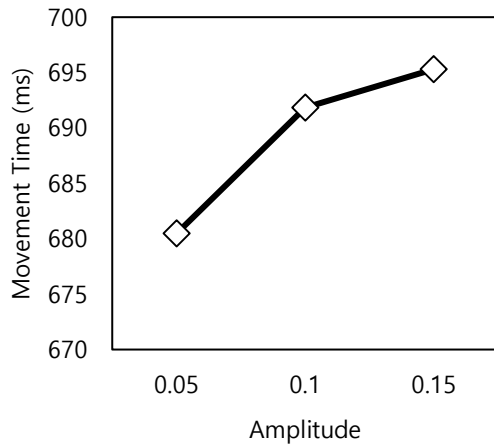
3.1. Fitts' Law

Movement time

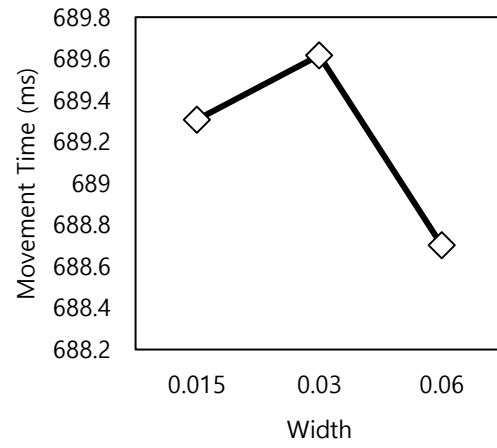
The average movement time as the function of amplitude, the width of the target, incline angle, and azimuth angles is shown in figure 13. The increase in amplitude increased the movement time as commonly known by the Fitts' Law concept; however, the width of the target showed a peculiar effect on movement time. As shown in figure 13 (b) the movement time increased by 0.31ms as the target width increased from 0.015m to 0.03m then dropped down by 0.91ms as the target size doubled up to 0.06. From what is known about Fitts' Law, the movement time was supposed to decrease as the target width increases, yet there was a small increment of movement time at 0.03m target width. However, the change in movement speed was very small ($< 1\text{ms}$). Further analysis is required to understand a deeper relationship between target width and movement time.

Incline angle showed a similar pattern as the target width; the movement speed was smaller when the target was in the same x-z plane with the starting point, then increased by 3.64 ms at an angle of 30° , then drops down 0.93 ms as the angle increased to 60° . The change in movement speed by the levels of target width and incline angle showed a similar pattern, implying that the target size may have caused confusion on depth perception or vice versa. The correlation between the target width and incline angle (depth of target) needs to be further analyzed.

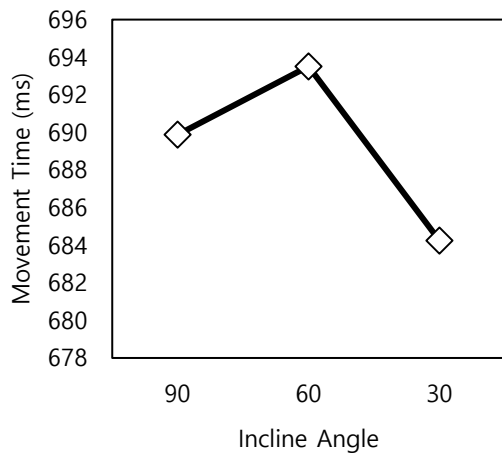
As for the azimuth angle, the study of Cha & Myung (2013) shows a sinusoidal pattern between the movement time and azimuth angle, however, in this study the movement time vs. azimuth angle plot does not show a strong sinusoidal pattern.



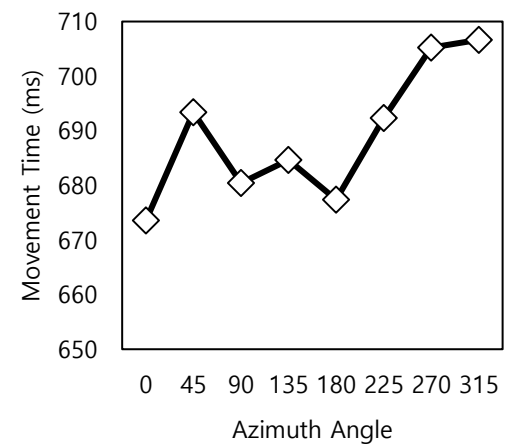
(a)



(b)



(c)



(d)

Figure 13. Average movement time as a function of (a) amplitude, (b) target width, (c) incline angle, and (d) azimuth angle.

The Fitts' Law model was developed using each trial data as well as the whole data to see how muscle fatigue affected the Fitts' Law model and each variable. The movement times of all participants were averaged by the same treatments (a total of 216 movement times were used for analysis). The regression model on the data from each trial of experiment returned the following Fitts' Law models. The parameter estimates and the p-values of each parameter from an effect test are shown in Table 2. Only the intercept showed a significant result on all models and the other parameters that showed significant results were the index of difficulty (trial 2) and the sigmoid of azimuth angle (Overall).

Trial 1

$$MT = 676.06 + 21.07 \left(\frac{1}{1 + e^{(-12\theta_2+6)}} \right) - 18.5 \cos(\theta_1) - 2.86ID \quad (8)$$

Trial 2

$$MT = 711.77 + 8.62 \left(\frac{1}{1 + e^{(-12\theta_2+6)}} \right) - 10.12 \cos(\theta_1) + 8.44ID \quad (9)$$

Trial 3

$$MT = 630.83 + 22.6 \left(\frac{1}{1 + e^{(-12\theta_2+6)}} \right) + 11.45 \cos(\theta_1) + 6.2ID \quad (10)$$

Overall Trials

$$MT = 672.89 + 17.43 \left(\frac{1}{1 + e^{(-12\theta_2+6)}} \right) - 5.72 \cos(\theta_1) + 3.93ID \quad (11)$$

Table 2. Parameters estimates (a: intercept, b: sigmoid of azimuth angle, c: cosine of incline angle, d: index of difficulty) and the p-value from effect test of each parameter

<i>Parameter</i>	Trial 1		Trial 2		Trial 3		Overall	
	<i>Estimate</i>	<i>P-value</i>	<i>Estimate</i>	<i>P-value</i>	<i>Estimate</i>	<i>P-value</i>	<i>Estimate</i>	<i>P-value</i>
Intercept, a	676.06	<0.0001*	711.77	<0.0001*	630.83	<0.0001*	672.89	<0.0001*
Sigmoid(θ_2), b	21.07	0.1174	8.62	0.4821	22.6	0.1035	17.43	0.0378*
Cosine(θ_1), c	-18.5	0.1648	-10.12	0.4048	11.45	0.4038	-5.72	0.4903
Index of Difficulty, d	-2.86	0.5263	8.44	0.0418*	6.2	0.1837	3.93	0.164

3.2. Muscle Fatigue

Speed vs. accuracy

In order to visualize the basic effect of muscle fatigue, the average movement time of each trial and the average error occurrences of each participant per trial were plotted together in Figure 14 along with both subjective and physiological measures of muscle fatigue at each trial listed in Table 3. The decrease in movement time and the increase in error occurrences across trials are clearly shown in Figure 14, representing the relationship between speed and accuracy with the physical load (fatigue).

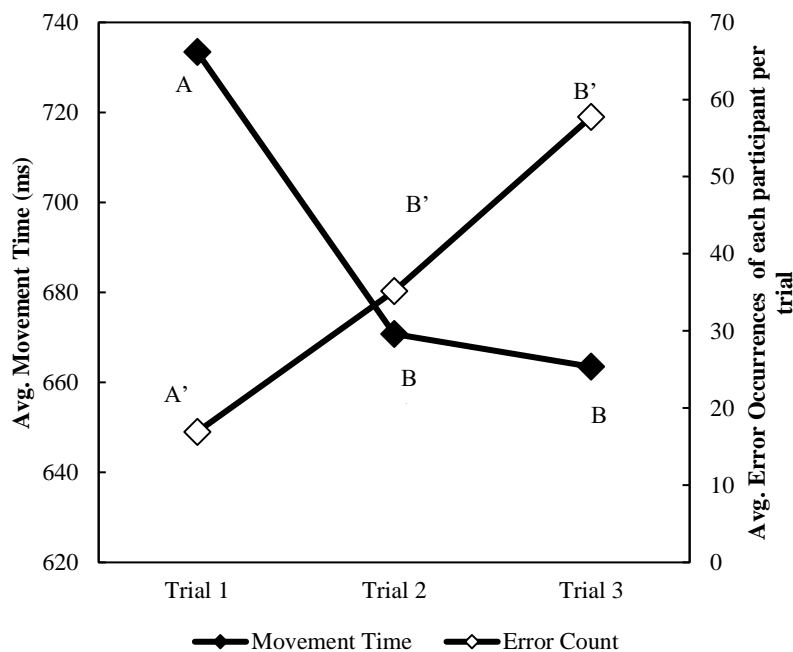


Figure 14. Average movement time vs. average error occurrence for each trial (A/B/C and A'/B'/C' are Tukey grouping results)

Muscle Fatigue

The subjective muscle fatigue of each trial was calculated by subtracting the Borg RPE Scale collected before the experiment begin from the scale collected after each trial, indicating how much the subjective muscle fatigue increased after each trial. Then the scale was averaged for each trial to observe the difference between the subject fatigue of bicep brachii and anterior deltoid. The median RMS value of each trial was divided by the median RMS value of the first 30 seconds to normalize (Park, Hong, & Lee, 2012), and then averaged by each trial for the same purpose as Borg RPE Scale data. The median frequency was then averaged as well as Borg RPE Scale and RMS percentage.

Table 3. Mean (SD) Borg RPE Scale, normalized RMS (median), and MDF (median) values of Bicep Brachii and Anterior Deltoid on each trial.

Fatigue Measures	Bicep Brachii			Anterior Deltoid		
	Trial 1	Trial 2	Trial 3	Trial 1	Trial 2	Trial 3
Borg RPE Scale (SD)	2.82 (2.34)	4.05 (2.08)	5.05 (2.20)	3.64 (2.16)	5.55 (2.11)	6.36 (1.86)
Normalized RMS (%)	1.45 (0.27)	1.39 (0.30)	1.39 (0.34)	2.82 (0.54)	4.05 (0.69)	5.05 (0.68)
MDF (Hz)	66.32 (16.74)	57.90 (14.81)	78.04 (72.29)	87.93 (27.97)	74.48 (15.44)	82.78 (39.58)

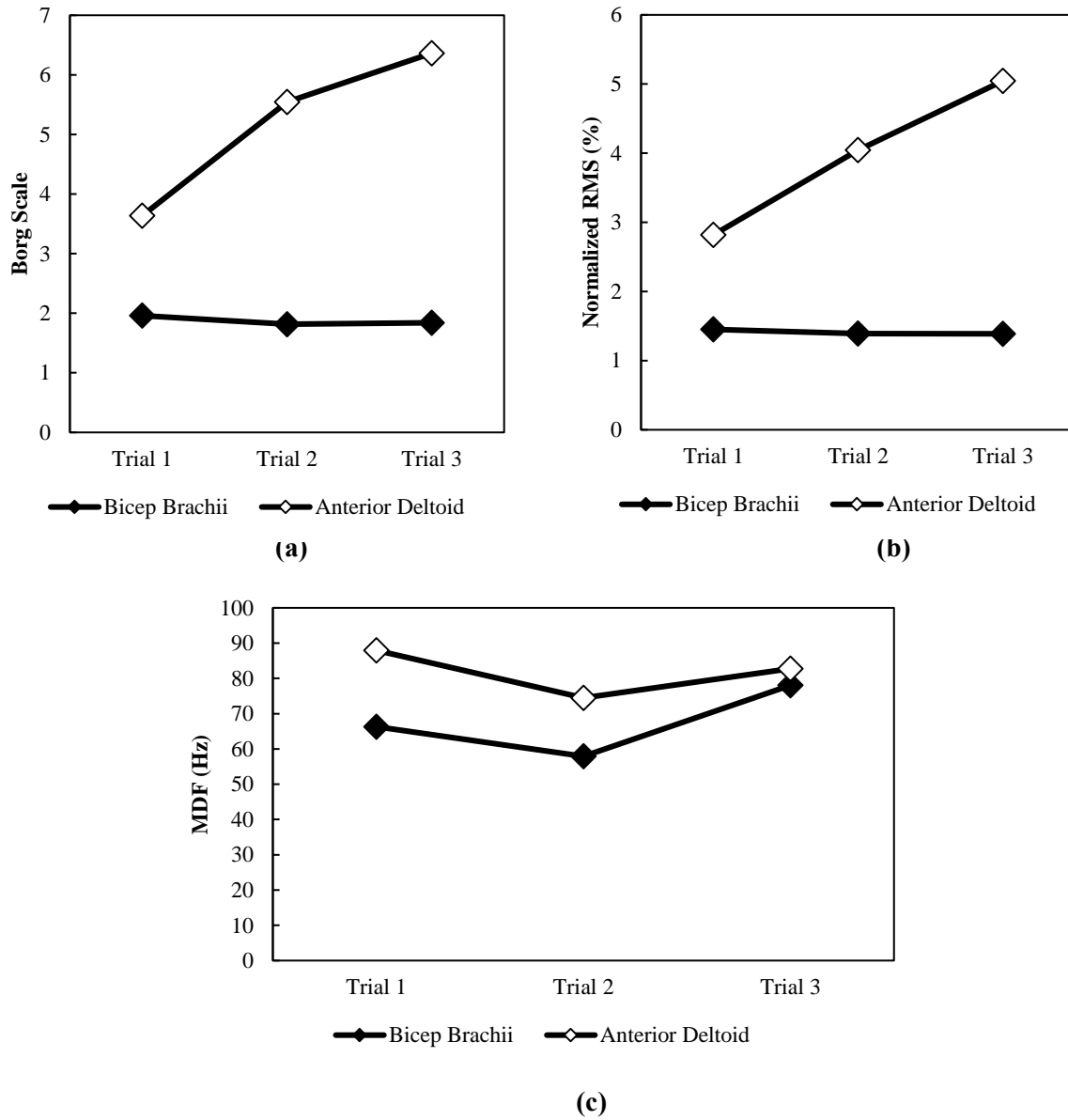


Figure 15. Fatigue of bicep brachii and anterior deltoid comparisons by (a) Borg RPE Scale, (b) normalized RMS, and (c) MDF

IV. Discussion

4.1 Fitts' Law

The Fitts' Law model developed using the result of this study showed a very low R^2 value compared to other previous 2D and 3D Fitts' Law models. Fitts (1966) represented the correlation between movement time and index of difficulty using the correlation coefficient r , which varied by the participant. However, when all data, averaged by the same ID, were plotted, the mean (SD) correlation coefficient was 0.96 (0.03) and 0.82 (0.12) even with different instructions applied (accuracy prioritized, speed prioritized, no priority). Cha & Myung (2013) have developed an extended 3D model including the sine of azimuth angle and incline angle with an R^2 of 0.85. For direct comparison with the results of Fitts (1966) and Cha & Myung (2013), the regression analysis with the same variables used in these previous studies was conducted. The regression model that was applied with only the ID as in the study of Fitts (1966) returned the model equation 12, with an R^2 of 0.003 and p-value of 0.16.

$$MT = 679 + 3.93ID \quad (12)$$

In comparison to Cha & Myung (2013), the sine of azimuth angle and unmodified incline angle value were used instead of sigmoid azimuth angle and cosine of incline angle; the result did not improve much by replacing the variables. However, the function of the azimuth angle returned a significant effect (p-value = 0.0378).

$$MT = 664.67 + 17.34\sin(\theta_2) + 5.4(\theta_1) + 3.93ID \quad (13)$$

Table 4. The post-hoc analysis result of the effect of the trial on movement time and error occurrence

Movement Time			Error Occurrence		
Level	Groups	Least Sq. Mean	Level	Groups	Least Sq. Mean
Trial 1	A	733.42	Trial 1	B'	16.92
Trial 2	B	670.73	Trial 2	B'	35.17
Trial 3	B	663.48	Trial 3	A'	57.75

4.1.1 Index of Difficulty

Index of Difficulty (ID) is the key variable of the Fitts Law. However, in this experiment even when the ID of difficulty was used alone to calculate the regression model, it failed to achieve significant R^2 value. ID only showed a significant effect on the model developed using data from the second trial. When compared with the original Fitts' work (Fitts, 1966) and the 3D model developed by Cha & Myung (2013), the parameters estimated for ID by both Fitts' original model and extended model by Cha had the same value of 3.93 as the model developed by using the overall data in this experiment (Equation 13), which indicates that ID has a constant effect on movement time whether used alone or with other variables. The effect of ID on movement time was examined using the average value of movement time for each index of difficulty (Figure 16). Figure 16 clearly shows the increasing trend of movement speed as the ID increases; however, there are unusual spikes at ID of 2.32 and 3.32 that may be caused by other variables. The range and scale of ID may cause the reason why ID had no significant role in predicting the movement time from the model developed in this experiment. Table 5 shows the level of width, amplitude, and ID with maximum and minimum ID used in the previous and current studies. Fitts used a wide range of ID (greater than or equal to 4 bits) further divided into narrow levels (less than 7 levels) for his study (Fitts, 1964, 1966), whereas Murata & Iwase (2001) and Cha & Myung (2013) used a narrow range of ID (less than 3 bits) but with wide levels (greater than 10 levels). However, in this study due to the narrow FOV of HTC Vive, the ID range was only 3.58 bits divided into 7 levels, which may have resulted in the non-significant effect of the ID.

Table 5. Index of difficulty levels and range comparison between current and previous Fitts' Law studies

Study	Width Level	Amplitude Levels	ID levels	Max. ID (bits)	Min. ID (bits)
Fitts (1964)	4	3	4	7	3
Fitts (1966)	3	3	6	7.58	2.58
Murata (2001)	4	4	16	5.65	3.1
Cha and Myung(2018)	3	4	12	5.84	3.87
Current Study	3	3	7	4.32	0.74

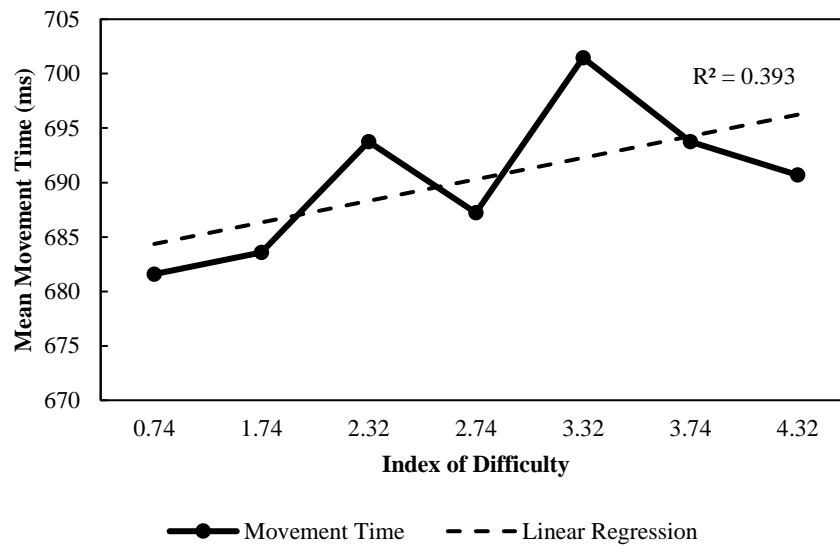


Figure 16. Regression of average movement time by the index of difficulty ($p = 0.104$)

4.1.2. Incline angle and target width

The graph on figure 13 (b) and (c) shows similar patterns between the target width and incline angle; however, the ANOVA result showed non-significant main and interaction effects of incline angle and target width (Table 6).

Table 6. ANOVA result to test the effect of incline angle and target width on movement time

Source	Nparm	DF	Sum of Squares	F Ratio	Prob > F
Incline Angle	2	2	9418.95	0.83	0.44
Width	2	2	93.35	0.008	0.99
Incline Angle*Width	4	4	10270.02	0.45	0.77

4.1.3. Azimuth angle

Azimuth angle, on the other hand, is the only variable that showed a significant effect on the Fitts' Law model using data from overall trials in both sigmoid function and sinusoidal function (Tables 2 & 7). However, the post hoc analysis of the azimuth angle showed significant differences between each level only for the sigmoid and the sinusoidal function of the azimuth angle (Table 8).

Table 7. Effect test result using the sinusoidal function of azimuth angle instead of sigmoid

Source	Nparm	DF	Sum of Squares	F Ratio	Prob > F
sin(Azimuth Angle)	1	1	24370.8	4.33	0.038*
cos(Incline Angle)	1	1	2679.8	0.48	0.49
ID(Fitts)	1	1	10920.3	1.94	0.16

Table 8. Tukey's HSD result on sinusoidal function and sigmoid function of azimuth angle (post hoc analysis)

The sinusoidal function of Azimuth Angle			The sigmoid function of Azimuth Angle		
Level	Group	Least Sq. Mean	Level	Group	Least Sq. Mean
0.5	A	695.34	0.5	A	695.34
1	A B	693.92	0.998	A B	693.92
0	B	676.57	0.002	B	676.57

Despite the effect test result indicating the significant result of azimuth angle in both sinusoidal and sigmoid functions, the movement time vs. azimuth angle plot shows neither sinusoidal nor sigmoidal pattern (Figure 17). Figure 17 shows the movement time at each azimuth angle at the different level of (a) incline angle, (b) amplitude, and (c) target width. Although none of them shows significant interactions with azimuth angle, (a) and (c) show that even though incline angle and target width show a similar pattern when plotted against movement time (Figure 13), they have different patterns respect to azimuth angle.

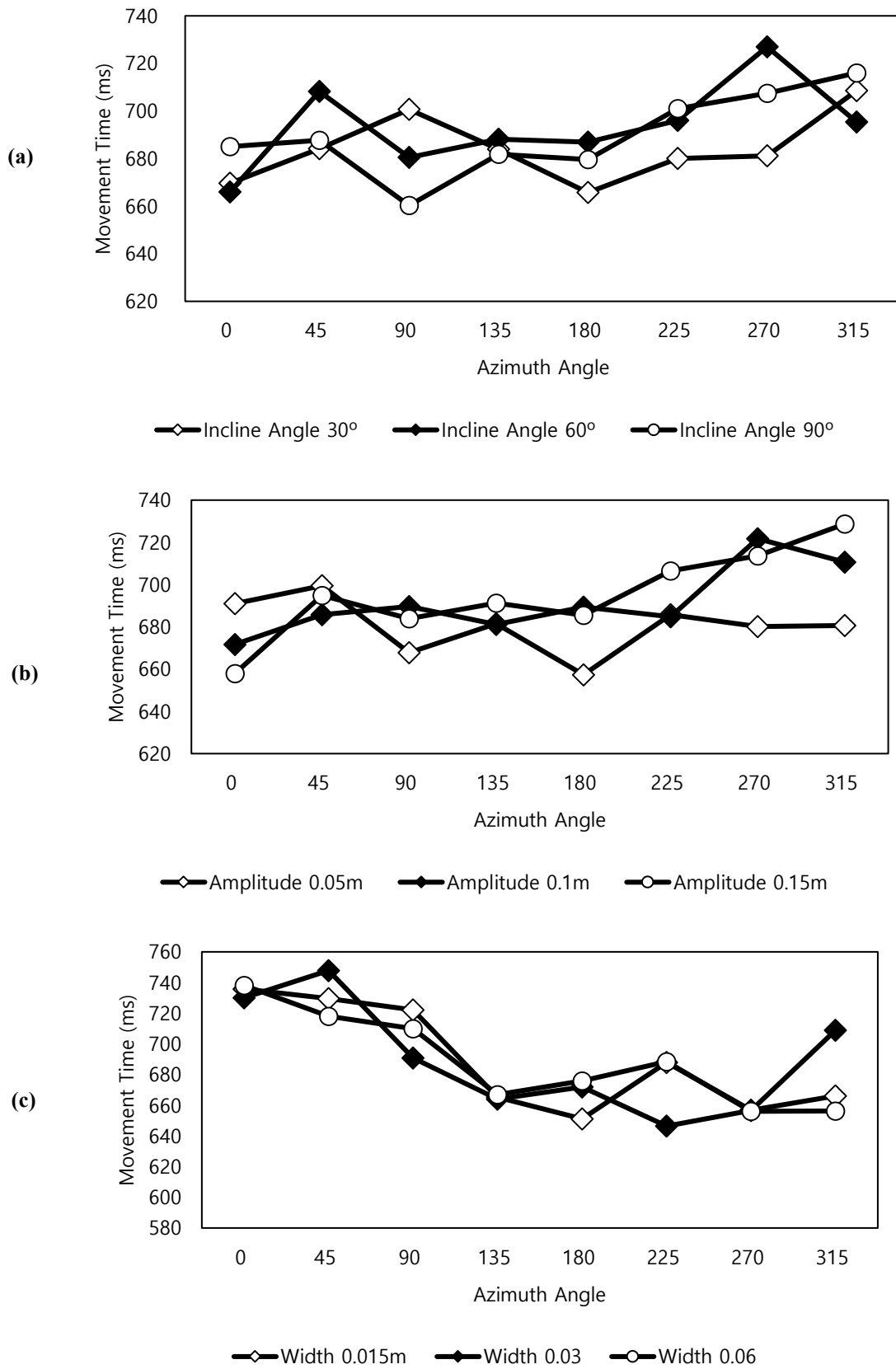


Figure 17. Movement time by azimuth angle at each level of (a) incline angle, (b) amplitude, and (c) target width

4.2 Muscle Fatigue

Figure 14 clearly shows the effect of trials on the movement time (speed) and error occurrence (accuracy). The regression analysis on the effect of trials on movement time and error occurrence showed significant effects by trial on both movement time ($p < 0.0001$) and error occurrence ($p < 0.0001$). The post-hoc analysis on trial showed significant differences between trial 1 and trial 2 or 3 in the case of movement time. For the error occurrence, trial 3 was significantly different from trial 1 and 2 (Table 4). The movement time significantly decreased as the second trial began, then there was not much change in trial 3, in the case of error occurrence. The number of errors increased significantly in trial 3. The prediction model by regression analysis of both movement time and error occurrence respect to trial is shown in equations 14 and 15. The slopes in equations 14 and 15 were opposite - a negative slope for movement time and a positive slope for error occurrence. Across trials, the movement speed increased, and the accuracy decreased.

$$MT = 759.15 - 34.97 \text{ Trial} \quad (14)$$

$$\text{Error Occurrence} = -3.09 + 19.68 \text{ Trial} \quad (15)$$

The increase in muscle fatigue was also observed by Borg RPE scale. Figure 15 (a) shows the subject fatigue building upon anterior deltoid, but not on bicep brachii, the same pattern is observed on normalized RMS data (Figure 15, b) as well (though not significant). The normalized RMS on anterior deltoid muscle increases as the number of trial increases while the normalized RMS of bicep brachii muscle stays the same. Meanwhile, the MDF calculated by FFT algorithm of both anterior deltoid and bicep brachii shows the interesting result (Figure 15, c). In most cases, the increase in fatigue results in the increase of amplitude domain parameter of EMG as well as the shift of median frequency to a lower value; however, such a reversed relation was not observed in this study. In the current study, RMS increased as the fatigue built up, whereas the frequencies shifted downward in trial 2 then upward in trial 3. Statistically, the significant effect of treatment exposure (trial number) on muscle fatigue was observed only for the perceived anterior deltoid and bicep brachii muscle fatigue rated on Borg's scale (Table 9). Similar results were observed for low-load static tasks (Öberg, Sandsjö, & Kadefors, 1994). In Öberg, Sandsjö, & Kadefors (1994), the physiological (objective) measure data (the MPF values) showed a significant effect when applied the high load tasks (holding 2 kg for 2.5 min), but not when applied on low load tasks (holding 0 kg for 5 min).

Table 9. ANOVA result on trial effect on muscle fatigue

Responses	Muscle Part	p-value
RMS	Bicep Brachii	0.095
RMS	Anterior Deltoid	0.37
MDF	Bicep Brachii	0.54
MDF	Anterior Deltoid	0.46
Borg's Scale	Bicep Brachii	<0.0001*
Borg's Scale	Anterior Deltoid	<0.0001*

Table 10. Post-hoc analysis of the trial effect on Borg's scale on bicep brachii

Level	Group	Least Sq. Mean
Trial 3	A	5.05
Trial 2	B	4.05
Trial1	C	2.82

Table 11. Post-hoc analysis of the trial effect on Borg's scale on anterior deltoid

Level	Group	Least Sq. Mean
Trial 3	A	6.36
Trial 2	A B	5.55
Trial 1	B	3.64

V. Conclusion

The 3 trials made a significant effect on the movement time and error rate of Fitts' Law task. However, all independent variables except the sinusoid and sigmoid function of azimuth angle failed to show a significant effect on the prediction of movement time using the Fitts' Law model. Although the sinusoid ($p = 0.038$) and sigmoid ($p = 0.038$) functions of azimuth angle showed a significant effect when all the trial data were compiled, but they showed non-significant effects for each trial. The index of difficulty only showed a glimpse of the possibility of its independence from other variables as it showed a constant parameter estimate when analyzed with sinusoid or sigmoid function of azimuth angle or when ID was analyzed alone. In conclusion, Fitts' law did not strongly hold in the virtual environment.

There are some limitations to this study. The failure of proving the applicability of Fitts' Law in the virtual environment points out the obvious problem of virtual reality itself, the fact that it is not the same as real life. In addition, the HMD used for this experiment, HTC Vive, is one of the most advanced VR HMD devices that can be found in the market; however, the resolution of the display is still sloppy with pixel lines visible with naked eyes and blur images outside of central vision to avoid vection and hence the unavoidable disadvantage of depth perception. In order to test multiple spectra of 3D Fitts' Law, this study used a limited ID range and neglected the depth perception capability test of HTC Vive. There is a possibility that participants have successfully acquired the target object by the tactile feedback rather than actually perceiving the depth or the position of the target. To overcome such limitations, the Fitts' Law test in the VR environment must return to basic and start with fundamental 2D tasks with a limited number of independent variables at a time to test the validity of each variable step by step. As for the muscle fatigue, a clear speed-accuracy tradeoff was observed under the influence of muscle fatigue; however, only the perceived anterior deltoid ($p < 0.0001$) and bicep brachii ($p < 0.0001$) muscle fatigues showed a significant result. When using a remote control like input device held with hands and controlled using an upper limb, the anterior deltoid is predominantly involved; however, there are other muscle parts (e.g., trapezius muscles) to be additionally involved. Furthermore, to successfully explain the effect of muscle fatigue on Fitts' Law, the muscle fatigue data must be included into Fitts' Law model as one of the variables. Finally, the Fitts' Law model developed in this study is a modified version of the extended Fitts' Law model by Cha & Myung (2013). To truly explain the 3D Fitts' Law and interpret the 3-dimensional positional data (not just amplitude) of a target into processable bits, it would be better to include extra parameters related to target position into the ID function.

References

- Ahlström, D. (2005, April). Modeling and improving selection in cascading pull-down menus using Fitts' law, the steering law and force fields. In *Proceedings of the SIGCHI conference on Human factors in computing systems* (pp. 61-70). ACM.
- Arsenault, R., & Ware, C. (2004). The importance of stereo and eye-coupled perspective for eye-hand coordination in fish tank VR. *Presence: Teleoperators & Virtual Environments*, 13(5), 549-559.
- Accot, J., & Zhai, S. (2003, April). Refining Fitts' law models for bivariate pointing. In *Proceedings of the SIGCHI conference on Human factors in computing systems* (pp. 193-200). ACM.
- Biocca, F. (1992). Virtual reality technology: A tutorial. *Journal of Communication*, 42(4), 23-72.
- Borg, G. (1998). Borg's perceived exertion and pain scales. *Human kinetics*.
- Cha, Y., & Myung, R. (2013). Extended Fitts' law for 3D pointing tasks using 3D target arrangements. *International Journal of Industrial Ergonomics*, 43(4), 350-355.
- Das, K., & Borst, C. W. (2010, March). An evaluation of menu properties and pointing techniques in a projection-based VR environment. In *3D User Interfaces (3DUI), 2010 IEEE Symposium on* (pp. 47-50). IEEE.
- Dichgans, J., & Brandt, T. (1978). Visual-vestibular interaction: Effects on self-motion perception and postural control. In *Perception* (pp. 755-804). Springer, Berlin, Heidelberg.
- Fitts, P. M. (1954). The information capacity of the human motor system in controlling the amplitude of movement. *Journal of experimental psychology*, 47(6), 381.
- HOFFMANN, E. R. (1995). Effective target tolerance in an inverted Fitts task. *Ergonomics*, 38(4), 828-836.
- Fitts, P. M., & Peterson, J. R. (1964). Information capacity of discrete motor responses. *Journal of experimental psychology*, 67(2), 103.
- Fitts, P. M., & Radford, B. K. (1966). Information capacity of discrete motor responses under different cognitive sets. *Journal of Experimental Psychology*, 71(4), 475.
- Hansen, J. P., Rajanna, V., MacKenzie, I. S., & Bækgaard, P. (2018, June). A Fitts' law study of click and dwell interaction by gaze, head and mouse with a head-mounted display. In *Proceedings of the Workshop on Communication by Gaze Interaction* (p. 7). ACM.
- Hoffmann, E. R. (1991). A comparison of hand and foot movement times. *Ergonomics*, 34(4), 397-406.
- Hoffmann, E. R. (1995). Effective target tolerance in an inverted Fitts task. *Ergonomics*, 38(4), 828-836.
- Johnsgard, T. (1994, May). Fitts' Law with a virtual reality glove and a mouse: Effects of gain. In *Graphics interface* (pp. 8-8). Canadian Information Processing Society.
- Kiryu, T., & So, R. H. (2007). Sensation of presence and cybersickness in applications of virtual reality for advanced rehabilitation.

- Konrad, P. (2005). The abc of emg. A practical introduction to kinesiological electromyography, 1, 30-35.
- Liu, L., van Liere, R., Nieuwenhuizen, C., & Martens, J. B. (2009, March). Comparing aimed movements in the real world and in virtual reality. In Virtual Reality Conference, 2009. VR 2009. IEEE (pp. 219-222). IEEE.
- Ma, L., Chablat, D., Bennis, F., & Zhang, W. (2009). A new simple dynamic muscle fatigue model and its validation. *International Journal of Industrial Ergonomics*, 39(1), 211-220.
- MacKenzie, I. S. (1992). Fitts' law as a research and design tool in human-computer interaction. *Human-computer interaction*, 7(1), 91-139.
- MacKenzie, I. S., & Ware, C. (1993, May). Lag as a determinant of human performance in interactive systems. In Proceedings of the INTERACT'93 and CHI'93 conference on Human factors in computing systems (pp. 488-493). ACM.
- Murata, A., & Iwase, H. (2001). Extending Fitts' law to a three-dimensional pointing task. *Human movement science*, 20(6), 791-805.
- Öberg, T, Sandsjö, L., & Kadefors, R. (1994). Subjective and objective evaluation of shoulder muscle fatigue. *Ergonomics*, 37(8), 1323-1333.
- Park, K. S., Hong, G. B., & Lee, S. (2012). Fatigue problems in remote pointing and the use of an upper-arm support. *International Journal of Industrial Ergonomics*, 42(3), 293-303.
- Pontonnier, C., Dumont, G., Samani, A., Madeleine, P., & Badawi, M. (2014). Designing and evaluating a workstation in real and virtual environment: toward virtual reality based ergonomic design sessions. *Journal on Multimodal User Interfaces*, 8(2), 199-208.
- Ramcharitar, A., & Teather, R. J. (2017, May). A Fitts' Law Evaluation of Video Game Controllers: Thumbstick, Touchpad and Gyro sensor. In Proceedings of the 2017 CHI Conference Extended Abstracts on Human Factors in Computing Systems (pp. 2860-2866). ACM.
- Sanchez-Vives, M. V., & Slater, M. (2005). From presence to consciousness through virtual reality. *Nature Reviews Neuroscience*, 6(4), 332.
- Schuemie, M. J., Van Der Straaten, P., Krijn, M., & Van Der Mast, C. A. (2001). Research on presence in virtual reality: A survey. *CyberPsychology & Behavior*, 4(2), 183-201.
- Slater, M., Usoh, M., & Steed, A. (1995). Taking steps: the influence of a walking technique on presence in virtual reality. *ACM Transactions on Computer-Human Interaction (TOCHI)*, 2(3), 201-219.
- Steuer, J. (1992). Defining virtual reality: Dimensions determining telepresence. *Journal of communication*, 42(4), 73-93.
- Teather, R. J., Natapov, D., & Jenkin, M. (2010, March). Evaluating haptic feedback in virtual environments using ISO 9241-9. In Virtual Reality Conference (VR), 2010 IEEE (pp. 307-308). IEEE.
- Troiano, A., Naddeo, F., Sossio, E., Camarota, G., Merletti, R., & Mesin, L. (2008). Assessment of force

- and fatigue in isometric contractions of the upper trapezius muscle by surface EMG signal and perceived exertion scale. *Gait & posture*, 28(2), 179-186.
- Ware, C., & Balakrishnan, R. (1994a). Reaching for objects in VR displays: lag and frame rate. *ACM Transactions on Computer-Human Interaction (TOCHI)*, 1(4), 331-356.
- Ware, C., & Balakrishnan, R. (1994b). Target acquisition in fish tank VR: The effects of lag and frame rate. In *Graphics Interface* (pp. 1-1). Canadian Information Processing Society.
- Ware, C., & Lowther, K. (1997). Selection using a one-eyed cursor in a fish tank VR environment. *ACM Transactions on Computer-Human Interaction (TOCHI)*, 4(4), 309-322.
- Welford, A. T. (1968). *Fundamentals of skill*.
- Welford, A. T. (1960). The measurement of sensory-motor performance: survey and reappraisal of twelve years' progress. *Ergonomics*, 3(3), 189-230.

